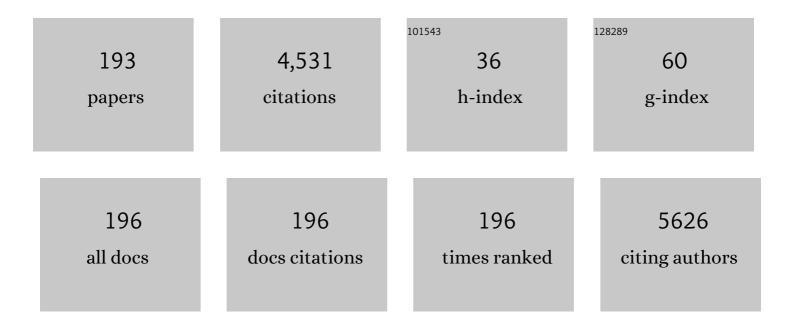
## List of Publications by Year in descending order

Source: https://exaly.com/author-pdf/7802483/publications.pdf Version: 2024-02-01



ALAY SINCH

#	Article	IF	CITATIONS
1	Self-Operating Flyback Converter for Boosting Ultra-Low Voltage of Thermoelectric Power Generator for IoT Applications. IEEE Transactions on Industrial Electronics, 2022, 69, 12957-12966.	7.9	6
2	Bismuth Telluride Based Efficient Thermoelectric Power Generator with Electrically Conducive Interfaces for Harvesting Low Temperature Heat. Journal of Science: Advanced Materials and Devices, 2022, , 100447.	3.1	3
3	Electromagnetic interference shielding effectiveness of polypyrrole-silver nanocomposite films on silane-modified flexible sheet. High Performance Polymers, 2022, 34, 310-320.	1.8	5
4	Synergistic effect of Zn doping on thermoelectric properties to realize a high figure-of-merit and conversion efficiency in Bi <sub>2â^²<i>x</i></sub> Zn <sub><i>x</i></sub> Te <sub>3</sub> based thermoelectric generators. Journal of Materials Chemistry C, 2022, 10, 7970-7979.	5.5	13
5	Phase Variation of Ultrathin WO <sub>3</sub> Electronâ€Transport Layer Prepared by Scalable Langmuir–Blodgett Technique to Boost Efficiency of Dye Sensitized Solar Cells. Solar Rrl, 2022, 6, .	5.8	3
6	Anionic conduction mediated giant n-type Seebeck coefficient in doped Poly(3-hexylthiophene) free-standing films. Materials Today Physics, 2021, 16, 100307.	6.0	11
7	A synergistic approach to achieving the high thermoelectric performance of La-doped SnTe using resonance state and partial band convergence. Materials Advances, 2021, 2, 4352-4361.	5.4	8
8	Carbon doping-induced defect centers in anodized alumina with enhanced optically stimulated luminescence. Journal of Materials Science: Materials in Electronics, 2021, 32, 10635-10643.	2.2	0
9	Radiation-resistant beta-photovoltaic battery using Ce-doped Gd3Ga3Al2O12 single-crystal scintillator. Applied Physics Letters, 2021, 118, .	3.3	5
10	High temperature Si–Ge alloy towards thermoelectric applications: A comprehensive review. Materials Today Physics, 2021, 21, 100468.	6.0	38
11	Flexible, Biocompatible PET Sheets: A Platform for Attachment, Proliferation and Differentiation of Eukaryotic Cells. Surfaces, 2021, 4, 306-322.	2.3	2
12	Free-standing flexible multiwalled carbon nanotubes paper for wearable thermoelectric power generator. Journal of Power Sources, 2020, 449, 227493.	7.8	38
13	Band Convergence and Phonon Scattering Mediated Improved Thermoelectric Performance of SnTe–PbTe Nanocomposites. ACS Applied Energy Materials, 2020, 3, 8882-8891.	5.1	7
14	Electron Beam Induced Tailoring of Electrical Characteristics of Organic Semiconductor Films. Chemistry Africa, 2020, 3, 571-592.	2.4	3
15	Near room temperature thermoelectrics: Ag2Se. AIP Conference Proceedings, 2020, , .	0.4	1
16	High energy electron beam induced improved thermoelectric properties of PEDOT:PSS films. Polymer, 2020, 202, 122645.	3.8	22
17	Remarkable Improvement of Thermoelectric Figure-of-Merit in SnTe through In Situ-Created Te Nanoinclusions. ACS Applied Energy Materials, 2020, 3, 7113-7120.	5.1	14
18	Stabilizing Thermoelectric Figureâ€ofâ€Merit of Superionic Conductor Cu <sub>2</sub> Se through W Nanoinclusions. Physica Status Solidi - Rapid Research Letters, 2020, 14, 2000102.	2.4	12

#	Article	IF	CITATIONS
19	Ambient-air fabrication with inorganic/polymer hole transport layer: Towards low cost perovskite solar cells. AIP Conference Proceedings, 2020, , .	0.4	0
20	Tailoring of thermoelectric properties in Bi2Te3 by varying the sintering temperature. AIP Conference Proceedings, 2020, , .	0.4	2
21	Environment friendly SnTe thermoelectrics: Material to device. AIP Conference Proceedings, 2020, , .	0.4	0
22	Low temperature processable crystalline WO3 Langmuir-Blodgett ultra-thin film as blocking layer in solar cells application. AIP Conference Proceedings, 2020, , .	0.4	0
23	Thermoelectric power generation from the perspective of conducting polymers. AIP Conference Proceedings, 2020, , .	0.4	0
24	Effect of tin on thermoelectric power factor of indium tin oxide. AIP Conference Proceedings, 2019, , .	0.4	1
25	Boosting thermoelectric power factor of free-standing Poly(3,4ethylenedioxythiophene):polystyrenesulphonate films by incorporation of bismuth antimony telluride nanostructures. Journal of Power Sources, 2019, 435, 226758.	7.8	21
26	Realization of High Thermoelectric FigureÂof Merit in GeTe by Complementary Co-doping of Bi and In. Joule, 2019, 3, 2565-2580.	24.0	175
27	Low temperature processable ultra-thin WO3 Langmuir-Blodgett film as excellent hole blocking layer for enhanced performance in dye sensitized solar cell. Electrochimica Acta, 2019, 318, 405-412.	5.2	19
28	Temperature Driven Unusual Reversible p―to n‶ype Conduction Switching in Bi 2 Te 2.7 Se 0.3. Physica Status Solidi - Rapid Research Letters, 2019, 13, 1900121.	2.4	3
29	Scalable free-standing polypyrrole films for wrist-band type flexible thermoelectric power generator. Energy, 2019, 176, 853-860.	8.8	27
30	Design and development of DC to DC voltage booster to integrate with PbTe/TAGS-85 based thermoelectric power generators. Materials Science for Energy Technologies, 2019, 2, 429-433.	1.8	8
31	Improving the Thermoelectric Performance of Tetrahedrally Bonded Quaternary Selenide Cu2CdSnSe4 Using CdSe Precipitates. Journal of Electronic Materials, 2019, 48, 2120-2130.	2.2	2
32	Optimization of Thermoelectric Properties of Mechanically Alloyed p-Type SiGe by Mathematical Modelling. Journal of Electronic Materials, 2019, 48, 649-655.	2.2	6
33	Lead sulphide: Low cost, abundant thermoelectrics. AIP Conference Proceedings, 2018, , .	0.4	1
34	Effect of ball milling time on thermoelectric properties of bismuth telluride nanomaterials. AIP Conference Proceedings, 2018, , .	0.4	4
35	Elucidating the mechanisms behind thermoelectric power factor enhancement of poly(3,4-ethylenedioxythiophene):poly(styrenesulfonate) flexible films. Vacuum, 2018, 153, 238-247.	3.5	14
36	Modeling of gate bias controlled NO2 response of the PCDTBT based organic field effect transistor. Chemical Physics Letters, 2018, 698, 7-10.	2.6	13

#	Article	IF	CITATIONS
37	Morphologyâ€Driven Sensitivity Enhancement of MEHâ€PPV Langmuirâ€Blodgett Films on Plastic Substrates for NO <sub>2</sub> Gas. ChemistrySelect, 2018, 3, 188-194.	1.5	3
38	Electron beam induced modifications in electrical properties of Poly(3,4-ethylenedioxythiophene):poly(styrenesulfonate) films. Vacuum, 2018, 152, 243-247.	3.5	5
39	Conductive polymers for thermoelectric power generation. Progress in Materials Science, 2018, 93, 270-310.	32.8	274
40	Enhanced thermoelectric figure-of-merit of p-type SiGe through TiO2 nanoinclusions and modulation doping of boron. Materialia, 2018, 4, 147-156.	2.7	17
41	Electron beam induced modifications of polyaniline silver nano-composite films: Electrical conductivity and H2S gas sensing studies. Radiation Physics and Chemistry, 2018, 153, 131-139.	2.8	23
42	Transition from n- to p-type conduction concomitant with enhancement of figure-of-merit in Pb doped bismuth telluride: Material to device development. Materials and Design, 2018, 159, 127-137.	7.0	39
43	Electron beam induced modifications in flexible biaxially oriented polyethylene terephthalate sheets: Improved mechanical and electrical properties. Materials Chemistry and Physics, 2017, 189, 237-244.	4.0	12
44	Enhanced Cl <sub>2</sub> sensitivity of cobalt-phthalocyanine film by utilizing a porous nanostructured surface fabricated on glass. RSC Advances, 2017, 7, 4135-4143.	3.6	22
45	Flexo-green Polypyrrole – Silver nanocomposite films for thermoelectric power generation. Energy Conversion and Management, 2017, 144, 143-152.	9.2	41
46	Tellurium-free thermoelectrics: Improved thermoelectric performance of n-type Bi 2 Se 3 having multiscale hierarchical architecture. Energy Conversion and Management, 2017, 145, 415-424.	9.2	37
47	Optimisation of electrical contact resistance in Bi0.5Sb1.5Te3 for development of thermoelectric generators. AIP Conference Proceedings, 2017, , .	0.4	1
48	Tailoring thermal conductivity in PbS by incorporation of copper for thermoelectric applications. AIP Conference Proceedings, 2017, , .	0.4	1
49	Nanostructured polypyrrole: enhancement in thermoelectric figure of merit through suppression of thermal conductivity. Materials Research Express, 2017, 4, 085007.	1.6	34
50	Electron beam modified zinc phthalocyanine thin films for radiation dosimeter application. Synthetic Metals, 2017, 231, 143-152.	3.9	12
51	Synthesis & tailoring the thermal conductivity of Sr doped Bi2Se3 thermoelectric material. AIP Conference Proceedings, 2017, , .	0.4	0
52	Synergetic effect of CuS@ZnS nanostructures on photocatalytic degradation of organic pollutant under visible light irradiation. RSC Advances, 2017, 7, 34366-34375.	3.6	40
53	Improved performance of dye sensitized solar cell via fine tuning of ultra-thin compact TiO 2 layer. Solar Energy Materials and Solar Cells, 2017, 170, 127-136.	6.2	36
54	Boosting thermoelectric performance of p-type SiGe alloys through in-situ metallic YSi2 nanoinclusions. Nano Energy, 2016, 27, 282-297.	16.0	79

#	Article	IF	CITATIONS
55	Polyanilineâ€Wrapped ZnO Nanorod Composite Films on Diazoniumâ€Modified Flexible Plastic Substrates. Macromolecular Chemistry and Physics, 2016, 217, 1136-1148.	2.2	8
56	Studies on different configurations of cobalt phthalocyanine based flexible organic field effect transistor. AIP Conference Proceedings, 2016, , .	0.4	0
57	Chemical synthesis and characterization of PdTe-Ag2Te nanowires heterostructure. AIP Conference Proceedings, 2016, , .	0.4	0
58	Study of thermal stability of Cu2Se thermoelectric material. AIP Conference Proceedings, 2016, , .	0.4	17
59	Improvement in thermoelectric power factor of mechanically alloyed p-type SiGe by incorporation of TiB2. AIP Conference Proceedings, 2016, , .	0.4	2
60	Broadband enhancement in absorption cross-section of N719 dye using different anisotropic shaped single crystalline silver nanoparticles. RSC Advances, 2016, 6, 48064-48071.	3.6	20
61	Nanostructured Boron Nitride With High Water Dispersibility For Boron Neutron Capture Therapy. Scientific Reports, 2016, 6, 35535.	3.3	124
62	Key issues in development of thermoelectric power generators: High figure-of-merit materials and their highly conducting interfaces with metallic interconnects. Energy Conversion and Management, 2016, 114, 50-67.	9.2	231
63	Electron density profile at the interfaces of bulk heterojunction solar cells and its implication on the S-kink characteristics. Chemical Physics Letters, 2016, 646, 6-11.	2.6	15
64	High temperature thermoelectric performance of NiCr2Se4. AIP Conference Proceedings, 2015, , .	0.4	0
65	Cobalt phthalocyanine/ZnO nanowire heterojunction film for H2S sensor. AIP Conference Proceedings, 2015, , .	0.4	1
66	Enhanced H2S sensing characteristics of Au modified Fe2O3 thin films. Sensors and Actuators B: Chemical, 2015, 219, 125-132.	7.8	77
67	Fast Response and High Sensitivity of ZnO Nanowires—Cobalt Phthalocyanine Heterojunction Based H2S Sensor. ACS Applied Materials & Interfaces, 2015, 7, 17713-17724.	8.0	57
68	Flexible organic semiconductor thin films. Journal of Materials Chemistry C, 2015, 3, 8468-8479.	5.5	51
69	Interface mediated semiconducting to metallic like transition in ultrathin Bi2Se3 films on (100) SrTiO3 grown by molecular beam epitaxy. RSC Advances, 2015, 5, 87897-87902.	3.6	0
70	Micro-structural characterization of low resistive metallic Ni germanide growth on annealing of Ni-Ge multilayer. AIP Advances, 2015, 5, .	1.3	6
71	Room temperature detection of H2S by flexible gold–cobalt phthalocyanine heterojunction thin films. Sensors and Actuators B: Chemical, 2015, 206, 653-662.	7.8	59
72	Surface acoustic wave sensor based on nickel(II) phthalocyanine thin films for organophosphorous pesticides selective detection. , 2014, , .		4

#	Article	IF	CITATIONS
73	lodine doped polyaniline and cobalt-phthalocyanine as sensitive layers for ammonia detection via surface acoustic wave sensor. , 2014, , .		0
74	Thermoelectric properties of Ag added Ca0.98La0.02MnO3. , 2014, , .		3
75	Exfoliated clay/polyaniline nanocomposites through tandem diazonium cation exchange reactions and in situ oxidative polymerization of aniline. RSC Advances, 2014, 4, 65213-65222.	3.6	30
76	Ultrasensitive and Selective Detection of Dopamine Using Cobalt-Phthalocyanine Nanopillar-Based Surface Acoustic Wave Sensor. ACS Applied Materials & Interfaces, 2014, 6, 22378-22386.	8.0	30
77	Surface and interface physicochemical aspects of intercalated organo-bentonite. International Journal of Adhesion and Adhesives, 2014, 50, 204-210.	2.9	43
78	High thermoelectric performance of (AgCrSe <sub>2</sub> ) <sub>0.5</sub> (CuCrSe <sub>2</sub> ) <sub>0.5</sub> nano-composites having all-scale natural hierarchical architectures. Journal of Materials Chemistry A, 2014, 2, 17122-17129.	10.3	82
79	Enhanced Thermoelectric Properties of Selenium-Deficient Layered TiSe <sub>2–<i>x</i></sub> : A Charge-Density-Wave Material. ACS Applied Materials & Interfaces, 2014, 6, 18619-18625.	8.0	21
80	Structural and Magnetic Depth Profiling and Their Correlation in Self-Assembled Co and Fe Based Phthalocyanine Thin Films. Journal of Physical Chemistry C, 2014, 118, 4072-4077.	3.1	8
81	In Situ Diazonium-Modified Flexible ITO-Coated PEN Substrates for the Deposition of Adherent Silver–Polypyrrole Nanocomposite Films. Langmuir, 2014, 30, 9397-9406.	3.5	28
82	Thermoelectric performance of layered Sr <sub>x</sub> TiSe <sub>2</sub> above 300 K. Journal of Physics Condensed Matter, 2014, 26, 445002.	1.8	5
83	Improved thermoelectric performance of hot pressed nanostructured n-type SiGe bulk alloys. Journal of Materials Chemistry A, 2014, 2, 6922.	10.3	145
84	Core/shell, protuberance-free multiwalled carbon nanotube/polyaniline nanocomposites via interfacial chemistry of aryl diazonium salts. Journal of Colloid and Interface Science, 2014, 418, 185-192.	9.4	47
85	Flexible H2S sensor based on gold modified polycarbazole films. Sensors and Actuators B: Chemical, 2014, 200, 227-234.	7.8	78
86	H2S sensing using in situ photo-polymerized polyaniline–silver nanocomposite films on flexible substrates. Organic Electronics, 2014, 15, 71-81.	2.6	102
87	Influence of Cu intercalation on thermal transport properties of titanium diselenide. , 2013, , .		1
88	One step synthesis of highly ordered free standing flexible polypyrrole-silver nanocomposite films at air–water interface by photopolymerization. RSC Advances, 2013, 3, 13329.	3.6	56
89	Improved Thermoelectric Properties of Se-Doped n-Type PbTe1â^'x Se x (0Â≤xÂ≤1). Journal of Electronic Materials, 2013, 42, 2292-2296.	2.2	14
90	Bending stress induced improved chemiresistive gas sensing characteristics of flexible cobalt-phthalocyanine thin films. Applied Physics Letters, 2013, 102, .	3.3	38

#	Article	IF	CITATIONS
91	Charge transport and ammonia sensing properties of flexible polypyrrole nanosheets grown at air–liquid interface. Materials Chemistry and Physics, 2013, 140, 300-306.	4.0	14
92	Growth of Pd4S, PdS and PdS2 films by controlled sulfurization of sputtered Pd on native oxide of Si. Thin Solid Films, 2013, 539, 41-46.	1.8	35
93	Novel, ternary clay/polypyrrole/silver hybrid materials through in situ photopolymerization. Colloids and Surfaces A: Physicochemical and Engineering Aspects, 2013, 439, 193-199.	4.7	36
94	Electrochemical investigation of free-standing polypyrrole–silver nanocomposite films: a substrate free electrode material for supercapacitors. RSC Advances, 2013, 3, 24567.	3.6	55
95	CuCrSe2: a high performance phonon glass and electron crystal thermoelectric material. Journal of Materials Chemistry A, 2013, 1, 11289.	10.3	85
96	Chemiresistive gas sensing properties of nanocrystalline Co3O4 thin films. Sensors and Actuators B: Chemical, 2013, 176, 38-45.	7.8	74
97	Room temperature ammonia sensor based on jaw like bis-porphyrin molecules. Organic Electronics, 2013, 14, 1189-1196.	2.6	26
98	Nano-crystalline Fe2O3 thin films for ppm level detection of H2S. Sensors and Actuators B: Chemical, 2013, 181, 471-478.	7.8	110
99	Low temperature thermoelectric properties of Cu intercalated TiSe2: a charge density wave material. Applied Physics A: Materials Science and Processing, 2013, 111, 465-470.	2.3	24
100	One-step UV-induced modification of cellulose fabrics by polypyrrole/silver nanocomposite films. Journal of Colloid and Interface Science, 2013, 393, 130-137.	9.4	49
101	Photo-induced synthesis of polypyrrole-silver nanocomposite films on N-(3-trimethoxysilylpropyl)pyrrole-modified biaxially oriented polyethylene terephthalate flexible substrates. RSC Advances, 2013, 3, 5506.	3.6	76
102	Thermal transport properties of strontium intercalated titanium diselenide. , 2013, , .		1
103	Effect of hot-press sintering temperature on thermal transport properties of TiSe[sub 2]. , 2013, , .		2
104	Thermoelectric properties of CuCrSe[sub 2]. , 2013, , .		2
105	Growth and Electrical Transport Properties of Organic Semiconductor Thin Films. Solid State Phenomena, 2013, 209, 1-5.	0.3	2
106	Trap Free Space Charge Limited Conduction and High Mobility in Cobalt Phthalocyanine - Iron Phthalocyanine Composite Thin Films. Solid State Phenomena, 2013, 209, 52-56.	0.3	2
107	Thermoelectric performance of Cu intercalated layered TiSe2 above 300 K. Journal of Applied Physics, 2013, 114, .	2.5	17
108	Enhanced H[sub 2]S response of Au modified Fe[sub 2]O[sub 3] thin films. , 2013, , .		2

7

#	Article	IF	CITATIONS
109	Enhanced figure of merit in (AgCrSe[sub 2])[sub 0.75](CuCrSe[sub 2])[sub 0.25]. AIP Conference Proceedings, 2013, , .	0.4	1
110	Dramatic thermal conductivity reduction in PbSe[sub 0.5]Te[sub 0.5]. , 2013, , .		0
111	Electron accumulation/depletion at F[sub 16]CoPc/Znq[sub 3] heterojunction: Kelvin probe and charge transport study. , 2013, , .		0
112	16S rRNA and Omp31 Gene Based Molecular Characterization of Field Strains ofB. melitensisfrom Aborted Foetus of Goats in India. Scientific World Journal, The, 2013, 2013, 1-7.	2.1	10
113	Polypyrrole/Ag Nanocomposite Films on Diazonium Salt Modified Indium Tin Oxide Substrate. Journal of Colloid Science and Biotechnology, 2013, 2, 200-210.	0.2	7
114	Comparative H <sub>2</sub> S Sensing Characteristics of Fe <sub>2</sub> O <sub>3</sub> : Thin Film vs. Bulk. Soft Nanoscience Letters, 2013, 03, 6-8.	0.8	4
115	Synthesis and characterization of sol-gel derived Cr2O3 nanoparticles. AIP Conference Proceedings, 2012, , .	0.4	9
116	Reverse rectification behavior of NiPc (p-type)/F16CuPc (n-type) heterojunction. , 2012, , .		0
117	Improved thermoelectric properties of PbTe0.5Se0.5. , 2012, , .		0
118	Metal–semiconductor transition in ultrathin cobalt-phthalocyanine films grown on SrTiO3single crystal substrates. Applied Physics Letters, 2012, 100, 162101.	3.3	1
119	Flexible cobalt-phthalocyanine thin films with high charge carrier mobility. Applied Physics Letters, 2012, 101, .	3.3	11
120	Effect of Te doping on the thermopower of PbSe <sub>1–x</sub> Te <sub>x</sub> . Emerging Materials Research, 2012, 1, 306-311.	0.7	5
121	Thermoelectric properties of transition metal intercalated layered TiSe2. , 2012, , .		1
122	Fluorinated copper-phthalocyanine/cobalt-phthalocyaine organic heterojunctions: Charge transport and Kelvin probe studies. Applied Physics Letters, 2012, 100, .	3.3	9
123	Chemi-resistive gas sensing properties of cobalt-phthalocyanine / iron-phthalocyanine composite films. , 2012, , .		0
124	Implication of molecular orientation on charge transport and gas sensing characteristics of cobalt–phthalocyanine thin films. Organic Electronics, 2012, 13, 2600-2604.	2.6	16
125	Thermoelectric properties of AgCrSe2. AIP Conference Proceedings, 2012, , .	0.4	5
126	Enhanced Cl2 response of ultrathin bi-nuclear (cobalt–iron) phthalocyanine films. Sensors and Actuators B: Chemical, 2012, 171-172, 423-430.	7.8	8

#	Article	IF	CITATIONS
127	Defect profiling in organic semiconductor multilayers. Organic Electronics, 2012, 13, 1409-1419.	2.6	16
128	Influence of adsorbed oxygen on charge transport and chlorine gas-sensing characteristics of thin cobalt phthalocyanine films. Chemical Papers, 2012, 66, .	2.2	3
129	Metallic-like conduction in Co-phthalocyanine/Fe-phthalocyanine composite films grown on sapphire substrates. Applied Physics Letters, 2011, 99, .	3.3	12
130	Charge transport in ultrathin iron-phthalocyanine thin films under high electric fields. Journal of Physics Condensed Matter, 2011, 23, 355801.	1.8	1
131	Study of interfaces in organic semiconductor heterojunctions. Journal of Physics: Conference Series, 2011, 262, 012036.	0.4	Ο
132	Mechanism of Charge Transport in Cobalt and Iron Phthalocyanine Thin Films Grown by Molecular Beam Epitaxy. , 2011, , .		0
133	Temperature dependent H2S and Cl2 sensing selectivity of Cr2O3 thin films. Sensors and Actuators B: Chemical, 2011, 157, 466-472.	7.8	53
134	Improved charge conduction in cobalt-phthalocyanine thin films grown along 36.8Ű boundary of SrTiO3 bicrystals. Applied Physics Letters, 2011, 98, .	3.3	9
135	Thermoelectric Properties of Ca[sub 4]Mn[sub 3â^`x]Nb[sub x]O[sub 10]. , 2011, , .		1
136	Ordering Induced Enhancement of Charge Carrier Mobility In CoPc Thin Films. , 2011, , .		0
137	Implication of Structural Disorder in The Charge Transport Properties of Cobalt-phthalocyanine Thin Films. , 2011, , .		Ο
138	Role of structural disorder in charge transport properties of cobalt phthalocyanine thin films grown by molecular-beam epitaxy. Organic Electronics, 2010, 11, 1835-1843.	2.6	18
139	Bis-porphyrin films as ppb level chemiresistive sensors. Chemical Physics Letters, 2010, 488, 27-31.	2.6	19
140	Bias and temperature dependent charge transport in high mobility cobalt-phthalocyanine thin films. Applied Physics Letters, 2010, 96, .	3.3	29
141	Electrical And Positron Study Of The Interface Of Organic Semiconductor Heterojunction. , 2010, , .		0
142	Charge Transport Characteristics Of Cobalt Phthalocyanine Thin Films Grown By Molecular Beam Epitaxy. , 2010, , .		0
143	Spintronics in metallic superconductor/ferromagnet hybrid structures. International Journal of Materials Research, 2010, 101, 164-174.	0.3	2
144	Room temperature ppb level Cl2 sensing using sulphonated copper phthalocyanine films. Talanta, 2010, 82, 1485-1489.	5.5	31

#	Article	IF	CITATIONS
145	Charge transport in polypyrrole:ZnO-nanowires composite films. Applied Physics Letters, 2009, 95, 202106.	3.3	16
146	Development of low resistance electrical contacts for thermoelectric devices based on n-type PbTe and p-type TAGS-85 ((AgSbTe <sub>2</sub> ) <sub>0.15</sub> (GeTe) <sub>0.85</sub> ). Journal Physics D: Applied Physics, 2009, 42, 015502.	2.8	73
147	NO2 sensors with room temperature operation and long term stability using copper phthalocyanine thin films. Sensors and Actuators B: Chemical, 2009, 143, 246-252.	7.8	72
148	Study of iron phthalocyanine organic semiconductor thin films using slow positron beam. Physica Status Solidi C: Current Topics in Solid State Physics, 2009, 6, 2589-2591.	0.8	3
149	Parts-per-billion level chlorine sensors with fast kinetics using ultrathin cobalt phthalocyanine films. Chemical Physics Letters, 2009, 480, 185-188.	2.6	35
150	Temperature Dependent Current–Voltage Characteristics of Iron-Phthalocyanine Thin Films. Journal of Nanoscience and Nanotechnology, 2009, 9, 5262-5267.	0.9	2
151	Molecular Beam Epitaxy Growth of Iron Phthalocyanine Nanostructures. , 2009, , .		1
152	Proton transfer with a twist? Femtosecond Dynamics of 7â€(2â€pyridyl)indole in Condensed Phase and in Supersonic Jets. Angewandte Chemie - International Edition, 2008, 47, 6037-6040.	13.8	54
153	Growth of iron phthalocyanine nanoweb and nanobrush using molecular beam epitaxy. Physica E: Low-Dimensional Systems and Nanostructures, 2008, 41, 154-163.	2.7	39
154	Melt processing of alumina in graphite ambient for dosimetric applications. Journal of Luminescence, 2008, 128, 445-450.	3.1	14
155	Oxygen induced hysteretic current-voltage characteristics of iron-phthalocyanine thin films. Journal of Applied Physics, 2008, 104, .	2.5	21
156	Low temperature thermopower and electrical transport in misfit Ca3Co4O9with elongatedc-axis. Journal Physics D: Applied Physics, 2008, 41, 085414.	2.8	11
157	xmlns:mml="http://www.w3.org/1998/Math/MathML" display="inline"> <mml:mrow><mml:msub><mml:mi mathvariant="normal"&gt;Mn<mml:mn>5</mml:mn></mml:mi </mml:msub><mml:msub><mml:mi mathvariant="normal"&gt;Si<mml:mn>3</mml:mn></mml:mi </mml:msub><mml:msub><mml:mi mathvariant="normal"&gt;C<mml:mi>x</mml:mi></mml:mi </mml:msub></mml:mrow> films.	3.2	22
158	Physical Review B, 2008, 77, . Low current induced electroresistance in the polycrystalline La0.6Pb0.4MnO3 thin films. Journal of Applied Physics, 2007, 102, 043907.	2.5	4
159	Superconducting spin switch with perpendicular magnetic anisotropy. Physical Review B, 2007, 75, .	3.2	49
160	Spin-polarized current versus stray field in a perpendicularly magnetized superconducting spin switch. Applied Physics Letters, 2007, 91, 152504.	3.3	35
161	Mode-Selective Excited-State Proton Transfer in 2-(2â€~-Pyridyl)pyrrole Isolated in a Supersonic Jet. Journal of the American Chemical Society, 2007, 129, 2738-2739.	13.7	61
162	Structure and Photophysics of 2-(2â€~-Pyridyl)benzindoles:  The Role of Intermolecular Hydrogen Bonds. Journal of Physical Chemistry A, 2007, 111, 11400-11409.	2.5	22

#	Article	IF	CITATIONS
163	Ground and excited state vibrations of 2-(2′-pyridyl)pyrrole. Journal of Molecular Structure, 2007, 844-845, 286-299.	3.6	9
164	Magneto-transport properties of nano-crystalline and poly-crystalline La0.6Pb0.4MnO3 thin films. Journal of Magnetism and Magnetic Materials, 2007, 313, 115-121.	2.3	5
165	Manipulating superconductivity in perpendicularly magnetized FSF triple layers. Applied Physics A: Materials Science and Processing, 2007, 89, 593-597.	2.3	6
166	ELECTROGRAFTING OF ORGANIC MONOLAYERS ON SILICON FOR MOLECULAR ELECTRONICS. , 2007, , .		0
167	7-Pyridylindoles:Â Synthesis, Structure, and Properties. Journal of Organic Chemistry, 2006, 71, 7611-7617.	3.2	25
168	Magneto-transport and ferromagnetic resonance studies of polycrystalline La0.6Pb0.4MnO3 thin films. Solid State Communications, 2006, 137, 456-461.	1.9	7
169	Correlation between extrinsic magnetoresistance and electroresistance in La0.6Pb0.4MnO3 thin films as revealed from current–voltage and ferromagnetic resonance studies. Solid State Communications, 2006, 138, 430-435.	1.9	3
170	Tunneling characteristics and resistivity behavior ofLa0.6Pb0.4MnO3grain boundaries. Physical Review B, 2006, 73, .	3.2	10
171	An alternative method of preparation of dosimetric grade α-Al2O3:C by vacuum-assisted post-growth thermal impurification technique. Radiation Measurements, 2005, 39, 277-282.	1.4	63
172	Anisotropic electrical transport studies of Ca3Co4O9 single crystals grown by the flux method. Journal of Crystal Growth, 2005, 277, 246-251.	1.5	33
173	Ferromagnetic resonance studies of nanocrystalline La0.6Pb0.4MnO3 thin films. Materials Letters, 2005, 59, 728-733.	2.6	14
174	Magnetization and magnetotransport studies of Y Ba2Cu3O7ÂÂ/La1ÂxPbxMnO3heterostructures. Superconductor Science and Technology, 2004, 17, 342-346.	3.5	5
175	Growth and morphology of the single crystals of thermoelectric oxide material NaxCoO2. Crystal Research and Technology, 2004, 39, 572-576.	1.3	10
176	In-plane and out-of-plane anisotropic magnetoresistances in La1 â^'xPbxMnO3thin films. Philosophical Magazine, 2003, 83, 3181-3191.	1.6	5
177	Positron annihilation studies in theMgB2superconductor. Physical Review B, 2002, 66, .	3.2	10
178	Andreev reflections on aMgB2superconductor. Physical Review B, 2002, 66, .	3.2	5
179	Iâ^'Vcharacteristic measurements to study the nature of the vortex state and dissipation inMgB2thin films. Physical Review B, 2002, 66, .	3.2	13
180	Anisotropy of critical current density inc-axis-orientedMgB2thin films. Physical Review B, 2002, 65, .	3.2	14

#	Article	IF	CITATIONS
181	Microwave absorption studies of MgB2 superconductor. Pramana - Journal of Physics, 2002, 58, 799-802.	1.8	0
182	Preparation and characterization of MgB2 superconductor. Pramana - Journal of Physics, 2002, 58, 867-870.	1.8	1
183	Effect of substrate temperature on electrical and magnetic properties of epitaxial La1â^'x Pb x MnO3 films. Pramana - Journal of Physics, 2002, 58, 1065-1067.	1.8	1
184	Colossal magnetoresistance in layered manganite Nd2â^'2x Sr1+2x Mn2O7 (0 ≤ ≤0.5). Pramana - Journal of Physics, 2002, 58, 1085-1088.	1.8	1
185	Effect of grain boundaries on paraconductivity of YBa 2 Cu 3 O x. Journal of Physics and Chemistry of Solids, 2002, 63, 1797-1803.	4.0	32
186	XPS and AFM investigations of annealing induced surface modifications of MgO single crystals. Journal of Crystal Growth, 2002, 236, 661-666.	1.5	120
187	Enhanced magnetoresistance in nanocrystalline La0.6Pb0.4MnO3 thin films. Journal of Crystal Growth, 2002, 244, 313-317.	1.5	10
188	Growth of epitaxial multilayers consisting of alternately stacked superconducting YBa2Cu3O7â^'δ and colossal magnetoresistive La1â^'xPbxMnO3 layers. Journal of Crystal Growth, 2002, 243, 134-142.	1.5	9
189	Synthesis and characterization of MgB2 superconductor. Physica C: Superconductivity and Its Applications, 2001, 363, 149-154.	1.2	23
190	Degradation behavior of MgB2 superconductor. Physica C: Superconductivity and Its Applications, 2001, 363, 208-214.	1.2	53
191	Magnetic field dependent microwave absorption studies on a MgB2superconductor. Superconductor Science and Technology, 2001, 14, 572-575.	3.5	18
192	Electron Beam Modified Organic Materials and their Applications. Solid State Phenomena, 0, 239, 72-97.	0.3	14
193	Synergistic manifestation of band and scattering engineering in single aliovalent Sb alloyed anharmonic SnTe alloy in concurrence with rule of parsimony. Materials Advances, 0, , .	5.4	4